β-Spectrin Is Colocalized with Both Voltage-gated Sodium Channels and Ankyrin$_G$ at the Adult Rat Neuromuscular Junction

S.J. Wood and C.R. Slater

School of Neurosciences, The Medical School, University of Newcastle upon Tyne NE2 4HH, United Kingdom

Abstract. Voltage-gated sodium channels (VGSCs) are concentrated in the depths of the postsynaptic folds at mammalian neuromuscular junctions (NMJs) where they facilitate action potential generation during neuromuscular transmission. At the nodes of Ranvier and the axon hillocks of central neurons, VGSCs are associated with the cytoskeletal proteins, β-spectrin and ankyrin, which may help to maintain the high local density of VGSCs. Here we show in skeletal muscle, using immunofluorescence, that β-spectrin is precisely colocalized with both VGSCs and ankyrin$_G$, the nodal isoform of ankyrin. In en face views of rat NMJs, acetylcholine receptors (AChRs), and utrophin immunolabeling are organized in distinctive linear arrays corresponding to the crests of the postsynaptic folds. In contrast, β-spectrin, VGSCs, and ankyrin$_G$ have a punctate distribution that extends laterally beyond the AChRs, consistent with a localization in the depths of the folds. Double antibody labeling shows that β-spectrin is precisely colocalized with both VGSCs and ankyrin$_G$ at the NMJ. Furthermore, quantification of immunofluorescence in labeled transverse sections reveals that β-spectrin is also concentrated in perijunctional regions, in parallel with an increase in labeling of VGSCs and ankyrin$_G$, but not of dystrophin. These observations suggest that interactions with β-spectrin and ankyrin$_G$ help to maintain the concentration of VGSCs at the NMJ and that a common mechanism exists throughout the nervous system for clustering VGSCs at a high density.

Segregation of ion channels into distinct domains of the plasma membrane is important for the function of many cells. A major issue for neurobiology is how integral membrane proteins, such as acetylcholine receptors (AChRs)[1] and voltage-gated sodium channels (VGSCs) become restricted to particular membrane domains rather than remaining freely mobile in the membrane. Association with the spectrin-based cytoskeleton represents one possible mechanism (for review see Bennett, 1990; Bennett and Gilligan, 1993). Spectrin was first characterized in red blood cells (RBCs) where anion exchanger channels in the membrane are linked through ankyrin and spectrin to the underlying actin cytoskeleton. A similar mechanism may contribute to ion channel localization in the nervous system.

One particularly important class of ion channels in excitable cells is the VGSCs, which are essential for the initiation of action potentials in most nerve and muscle cells. In the nervous system, VGSCs have been shown to be clustered at axon hillocks and initial segments (Wollner and Catterall, 1986; Angelides et al., 1988) where they are responsible for initiating action potentials, and at nodes of Ranvier in both peripheral and central neurons (Waxman and Ritchie, 1985; Kaplan et al., 1997) where they mediate saltatory conduction in myelinated axons. In skeletal muscle, electrophysiological studies using loose-patch voltage clamp recording have shown that VGSCs are nonuniformly distributed with high sodium current densities present at the neuromuscular junction (NMJ) and in the perijunctional region (Betz et al., 1984; Beam et al., 1985; Caldwell et al., 1986). These findings were subsequently confirmed by immunofluorescence studies (Angelides, 1986; Haimovich et al., 1987) and EM immunolabeling, which further revealed that VGSCs are concentrated in the depths of the postsynaptic folds and in the perisynaptic membrane, although excluded from the AChR-rich domain at the tops of the folds (Flucher and Daniels, 1989; Le Treut et al., 1990; Boudier et al., 1992). The presence of a high density of VGSCs at the NMJ is believed to lower the threshold for action potential generation (Wood and Slater, 1995) and to increase the safety factor for neuromuscular transmission (Wood and Slater, 1997).

There is considerable interest in the molecular mecha-

Address all correspondence to S.J. Wood's present address, Department of Physiology, School of Medical Sciences, University of Bristol, University Walk, Bristol BS8 1TD, UK. Tel.: 44-117-928-7821. Fax: 44-117-928-8923. E-mail: s.j.wood@bristol.ac.uk

1. *Abbreviations used in this paper*: AChRs, acetylcholine receptors; BgTx, bungarotoxin; ETA, epitrochleoanconeous; J, junctional; NMJ, neuromuscular junction; PJ, perijunctional; RBC, red blood cell; VGSC, voltage-gated sodium channel; XJ, extrajunctional.

nisms that account for VGSC clustering at sites of action potential generation. It has been suggested that interactions with ankyrin and spectrin may play a role in maintaining a high density of VGSCs (Srinivasan et al., 1988). Although originally described in RBCs, isoforms of both spectrin and ankyrin have been identified throughout the nervous system. Spectrin is a flexible rod-shaped protein made up of homologous α and β subunits (Bennett, 1990; Bennett and Gilligan, 1993). The β subunit contains both the actin-binding site at the NH_2 terminus and the ankyrin binding site in the midregion. An isoform of β-spectrin has been shown to be present at the NMJ and in extrajunctional muscle membrane (Bloch and Morrow, 1989; Bewick et al., 1992). Bewick et al. (1992) observed that the distribution of β-spectrin was quite distinct from that of AChRs, and suggested that β-spectrin was in fact localized to the troughs of the postsynaptic folds. Spectrin is a member of a family of structurally related cytoskeleton proteins including utrophin and the muscle-specific dystrophin. Whereas the function of these two proteins is as yet unclear, their distribution in muscle fibers is well described. Utrophin is associated with AChRs at the NMJ (Ohlendiek et al., 1991; Bewick et al., 1992) and is implicated in stabilizing AChR clusters at the tops of the postsynaptic folds (Apel and Merlie, 1995). On the other hand, dystrophin, like β-spectrin, is found throughout the muscle fiber membrane and is concentrated at the NMJ where it is thought to be localized in the depths of the folds (Sealock et al., 1991; Yeadon et al., 1991; Bewick et al., 1992). This localization raises the possibility that both β-spectrin and dystrophin may have a role in localizing VGSCs to the depths of the postsynaptic folds.

Ankyrins are a family of peripheral membrane proteins that have been shown to interact with both ion channels and β-spectrin. It is now clear that there are at least three separate genes encoding the ankyrin family of proteins (for review see Lambert and Bennett, 1993). The first members of the ankyrin family described were $ankyrin_B$, which is the major ankyrin in the nervous system, and $ankyrin_R$, which is present in RBCs and has a restricted distribution in the nervous system. More recently, a third ankyrin, $ankyrin_G$, has been described; it is the largest ankyrin found to date (Kordeli et al., 1995). An isoform of $ankyrin_G$ is present at the nodes of Ranvier and at the initial segment of axons in central neurons (Kordeli et al., 1990; Kordeli and Bennett, 1991; Kordeli et al., 1995; Kaplan et al., 1997), suggesting that $ankyrin_G$ mediates the interaction between VGSCs and spectrin in these regions. Using an antibody raised against RBCs, ankyrin immunoreactivity has been shown to be localized at the NMJ in the depths of the postsynaptic folds (Flucher and Daniels, 1989) suggesting that a similar interaction may account for the high density of VGSCs at the NMJ.

If $ankyrin_G$ and β-spectrin mediate VGSC clustering, then it would be expected that these three proteins would be codistributed. Whereas there is much evidence suggesting that the β-spectrin–ankyrin interaction is important for aggregating VGSCs in neurons, the in situ colocalization of these three proteins has not been explicitly demonstrated. Here we have used immunofluorescence labeling to ask whether, in skeletal muscle, β-spectrin is colocalized with both VGSCs and the isoform of ankyrin found at the nodes of Ranvier, $ankyrin_G$. For comparison with β-spectrin, we have also examined the distribution of the related cytoskeletal proteins utrophin and dystrophin to identify whether they are colocalized with VGSCs and $ankyrin_G$. This study is a prerequisite to developmental studies that may give insight into how distinct VGSC–cytoskeleton domains are assembled and maintained.

Materials and Methods

Tissues

Soleus muscles isolated from adult female rats (~200 g) were used throughout the experiments. For immunolabeling, the muscles were prepared in one of two ways. Whole muscles were lightly fixed in paraformaldehyde (0.5% wt/vol) for 30 min, and then washed in PBS. The muscles were then teased into small bundles of 5–15 fibers and permeabilized with Triton X-100 (1% vol/vol) in PBS for 30 min. These teased fibers, which allow NMJs to be viewed en face, were then immunolabeled as outlined below. Alternatively, muscles were prepared for cryosectioning by freezing blocks of muscle in isopentane cooled in liquid nitrogen. Transverse cryostat sections (6 μm) of the soleus muscles were cut and thaw mounted onto gelatine-coated slides. After air drying for 60 min, these slides were wrapped and stored at −40°C until required. Transverse cryosections of control and *mdx* mouse epitrochleoanconeous (ETA) muscles were similarly prepared.

Antibodies

The following primary antibodies were diluted in PBS containing 3% BSA and 0.1 M lysine as indicated. Two previously described monoclonal antibodies that recognize β-spectrin, raised against human RBC ghosts, were used. NCLSPEC2 was used in sections (1:30; Novacastra, Burlingame, CA) and RBC2/5C4 (Bewick et al., 1992) was used in teased fibers (1:2; a gift from Dr. L. Anderson, University of Newcastle upon Tyne). An affinity-purified rabbit polyclonal raised against peptides unique to the rat $ankyrin_G$ spectrin-binding domain Ank_G@SpBd was used in sections at 0.01 μg/μl and in teased fibers at 0.02 μg/μl (a gift from Dr. S. Lambert, Worcester Foundation for Biomedical Research, Shrewsbury, MA) (Kordeli et al., 1995). For VGSC labeling, a rabbit polyclonal antibody AP1380 raised against a synthetic peptide EOIII, which recognizes the highly conserved segment in the intracellular III–IV loop that is present in all known vertebrate sodium channels (a gift from Dr. R. Levinson, University of Colorado School of Medicine, Denver, CO) (Dugandzija-Novakovic et al., 1995) was used at a dilution of 1:30 in sections and 1:10 for teased fibers. Control experiments where the VGSC antibody (2 μl) was preabsorbed with the peptide antigen EOIII (1 μg in 1 μl) overnight at 4°C and then applied to the tissues revealed no significant labeling above the no primary control (Fig. 1). A monoclonal antibody DY8/6C5 to a COOH-terminal epitope of dystrophin was used at 1:50 in sections and at 1:10 in teased fibers (a gift from Dr. L. Anderson) (Bewick et al., 1992). A monoclonal antibody DRP3/20C5, raised against a fusion protein containing the first 261 NH_2-terminal amino acids of the utrophin sequence, was used at 1:10 in both sections and in teased fibers (a gift from Dr. L. Anderson) (also available as antibody NCLDRP2; Novacastra).

TRITC-conjugated swine anti–rabbit or rabbit anti–mouse IGs (Dako Ltd., High Wycombe, UK) were used as secondary antibodies in most experiments to recognize polyclonal and monoclonal primary antibodies, respectively. For double antibody–labeling experiments monoclonal primary antibodies were detected using a FITC-conjugated goat anti–mouse secondary (Dako Ltd.). All secondary antibodies were diluted at 1:100.

Immunolabeling

All incubations and washings were performed at room temperature except where stated and PBS was used for all washes.

Permeabilized, teased muscle fibers were incubated in primary antibodies overnight (at least 15 h) at 4°C. After allowing the fibers to warm to room temperature for 45 min, the bundles were washed for 45 min, and then incubated for 2 h in secondary antibodies. The secondary antibodies were preincubated with normal rat serum at a ratio of 2:1 for 1 h at room temperature before dilution. To enable NMJs to be identified, FITC α-bungarotoxin (BgTx) (6×10^{-7} M; Molecular Probes, Inc., Eugene, OR),

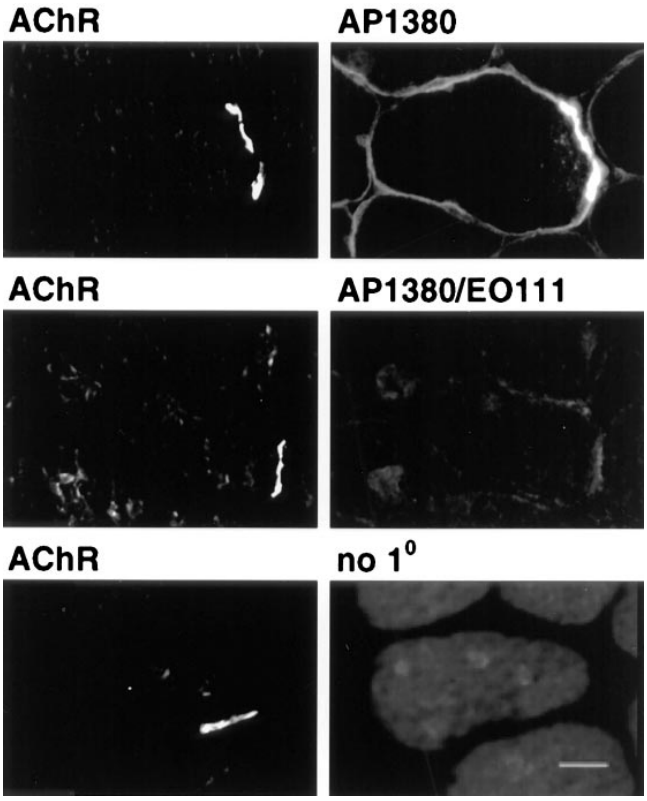

Figure 1. Specificity of immunolabeling of VGSCs. Digitized images of transverse sections of rat soleus muscle were dual labeled with FITC α-BgTx to identify AChRs at the NMJ and antibody to VGSCs (*AP1380*); antibody to VGSCs preincubated with the immunogenic peptide against which it was raised (*AP1380/EOIII*) or no primary antibody (diluent). All were visualized with TRITC secondary antibody. The images are printed so that the intensity levels in each column are comparable. Bar, 20 μm.

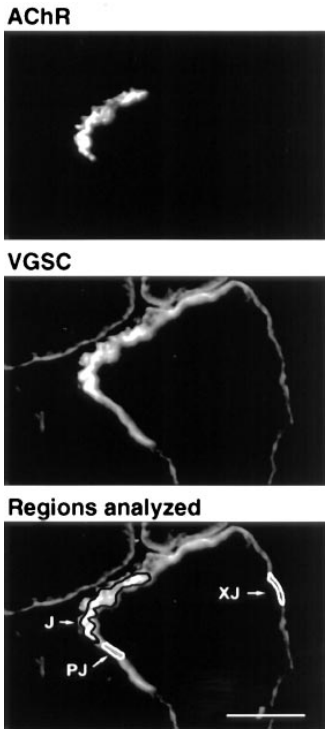

Figure 2. Identification of junctional (*J*), perijunctional (*PJ*), and extrajunctional (*XJ*) regions in immunolabeled transverse sections of rat soleus muscles. For analysis of immunofluorescence labeling intensity, sections were dual labeled with FITC α-BgTx to identify the AChRs at the NMJ and an antibody to the protein of interest, in this example polyclonal antibody to VGSCs (AP1380). Once J, PJ, and XJ regions were defined as described in the Materials and Methods, the mean fluorescence labeling intensity within each of them was determined. Bar, 20 μm.

which labels AChRs, was added with the secondary antibody solution. Subsequently, the fibers were washed (30 min), fixed in paraformaldehyde (1% wt/vol for 15 min), and then mounted on microscope slides in antifading fluorescence mounting medium (Vectashield; Vector Laboratories, Inc., Burlingame, CA). As a control, an identical labeling procedure was carried out with the omission of the primary antibody where diluent was applied instead.

Slide-mounted transverse sections were removed from the freezer and warmed to room temperature. Before labeling with primary antibodies, the unfixed sections were washed first with 0.1% Triton X-100 (vol/vol) for 5 min, and then washed for 15 min. The labeling procedure for sections and teased fibers was then essentially the same.

To examine the colocalization of proteins, double antibody labeling was performed with a monoclonal antibody to β-spectrin, dystrophin, or utrophin and a polyclonal antibody to either VGSCs or ankyrin$_G$ in both serial sections and in teased fiber preparations. Tissues were incubated in primary monoclonal antibodies for 6 h at 4°C, allowed to warm to room temperature, and washed as above. This was followed by incubation with FITC-conjugated goat anti–mouse for 2 h, a wash for 1 h, and then the primary polyclonal antibody was applied for 10 h at 4°C. Again the tissues were allowed to warm to room temperature, and were then washed before incubation with TRITC-conjugated swine anti–rabbit for 2 h. Finally the tissues were washed, fixed, and mounted as described above.

Microscopy

Double antibody–labeled transverse sections were photographed on an Optiphot-2 microscope using a ×40 oil Plan apo objective (Nikon UK Ltd., Kingston, UK). The rhodamine and fluorescein fluorescence were viewed with Nikon G-2A and B-2A filter sets, respectively. A525/20 nm bandpass emission filter (Leica UK Plc., Milkon Keynes, UK) was used to enhance the selectivity of the fluorescein images by preventing rhodamine "bleed through."

In addition, digitized images of labeled specimens were recorded using a cooled CCD camera imaging system (Astrocam, Cambridge, UK) and either a ×50 (Leitz) or a ×100 (Nikon) plan fluor oil immersion objectives on a M2B microscope (Micro Instruments Ltd., Oxford, UK) using Nikon filter blocks, G-1B (TRITC) and B-2H (FITC), with the additional narrow bandpass filter to improve fluorescein selectivity. All the digitized images were stored on optical disks for subsequent analysis using Imager 2+ software (Astrocam, Cambridge, UK) as outlined below.

To determine the localization of immunolabeling within the postsynaptic folds, double-labeled en face NMJs were also viewed with a confocal laser microscope (laser λ 488 nm for FITC; laser λ 568 nm for rhodamine) (MRC600; Bio-Rad Laboratories, Hercules, CA) using a ×60 objective (NA 1.4). NMJs were initially viewed en face. A line of interest was selected, through which a series of scans at different focal depths (0.3-μm steps) was made. From such series reconstructed transverse sections were produced. Subsequently, the entire NMJ was scanned in 10–15 steps of 0.5 μm to construct a complete en face view. The position of the transverse section was clearly identified in en face views where the fluorescence had been bleached.

Quantification

Images of both fluorescein and rhodamine labeling were recorded from transverse sections of muscle fibers that were dual labeled with a primary antibody to the protein of interest and with BgTx. The presence of FITC-α-BgTx binding to AChRs was used to identify the position of the NMJ (Fig. 2), and the corresponding rhodamine image demonstrates the presence of VGSC immunolabeling around the entire muscle fiber membrane. The intensity of fluorescence was measured in each of three regions of the muscle fiber surface (Fig. 2): the NMJ (*J*); the perijunctional region (*PJ*) immediately adjacent (0–5 μm) to the NMJ; and an extrajunctional region (*XJ*) diametrically opposed to the NMJ. For all the images obtained the camera was operating within a range where pixel intensity and exposure time were linearly related. All intensity values were expressed as gray levels per second of exposure time. The total fluorescence intensity within each region was calculated and the value obtained was divided by the area of the region to give the mean intensity of labeling per unit area. A background value determined by applying the same procedure to sections in which the primary antibody had been omitted was subtracted to give the

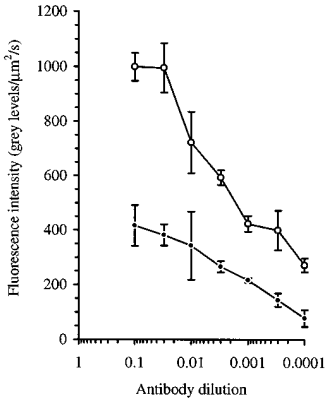

Figure 3. Example of the effect of antibody dilution on immunolabeling fluorescence intensity. Transverse cryostat sections of rat soleus muscle were dual labeled with an antibody against β-spectrin (NCLSPEC2), visualized with a TRITC secondary antibody, and with FITC α-BgTx to identify the NMJ. Each point is the mean (± SEM) fluorescence intensity in junctional (○) and extrajunctional (●) regions of six muscle fibers. For the β-spectrin antibody, the dilution at which most of the antigen binding sites are saturated is 1:30.

net labeling intensity. For each muscle fiber, the mean fluorescence intensity in J and PJ regions was normalized to that in the XJ region (assigned a value of 1). For each antibody, 10 muscle fibers in each of two soleus muscles were analyzed, and the results expressed as mean normalized fluorescence intensity ± SEM.

An important preliminary step in this quantification procedure was to establish an appropriate primary antibody dilution. If the fluorescence intensity is to be proportional to the number of protein molecules, then the primary antibodies should be used at or near saturating concentration. Using serial dilution experiments, an approximately saturating antibody concentration was determined for the primary antibodies to VGSC, ankyrin$_G$, β-spectrin, and dystrophin. Fig. 3 shows an example of a dilution series for the NCLSPEC2 antibody to β-spectrin. Muscle sections were exposed to serial dilutions of antibody and images containing NMJs were analyzed for J and XJ labeling as outlined above (without normalizing the labeling intensity to extrajunctional levels). The mean fluorescence labeling intensity per μm^2 in both J and XJ regions was plotted against antibody concentration (Fig. 3). Each point is the mean ± SEM of observations from six muscle fibers. The concentration at which the binding sites appeared saturated was used to label sections throughout the experiments. At this dilution, the greatest difference between labeling intensity in J and XJ regions of the muscle fiber can be seen.

Results

Distribution of VGSCs and Cytoskeletal Proteins at the NMJ

β-Spectrin, a cytoskeletal protein implicated in the maintenance of VGSC clusters throughout the nervous system, is concentrated at the NMJ (Bloch and Morrow, 1989; Bewick et al., 1992). To see whether it is well placed within the NMJ to interact with VGSCs, the distribution of both VGSCs and β-spectrin was examined using confocal microscopy (Fig. 4). Dual-labeled teased muscle fibers viewed en face show that both VGSCs and β-spectrin are approximately codistributed with AChRs at the NMJ (Fig. 4). The superimposed images show clearly that labeling for both VGSCs and β-spectrin extends laterally ~0.5 μm beyond that for AChRs. Bewick et al. (1993) reported that in en face views of NMJs a fringe of dystrophin or β-dystroglycan labeling could be seen to extend beyond AChR labeling. These authors interpreted this observed fringe of labeling as representing immunolabeling in the bottom of the postsynaptic folds.

To determine the localization of β-spectrin and VGSC immunolabeling within the postsynaptic folds, reconstructed transverse sections through the NMJ were produced. These images (Fig. 4) show that there are two discrete ion channel domains at the NMJ with AChR labeling and

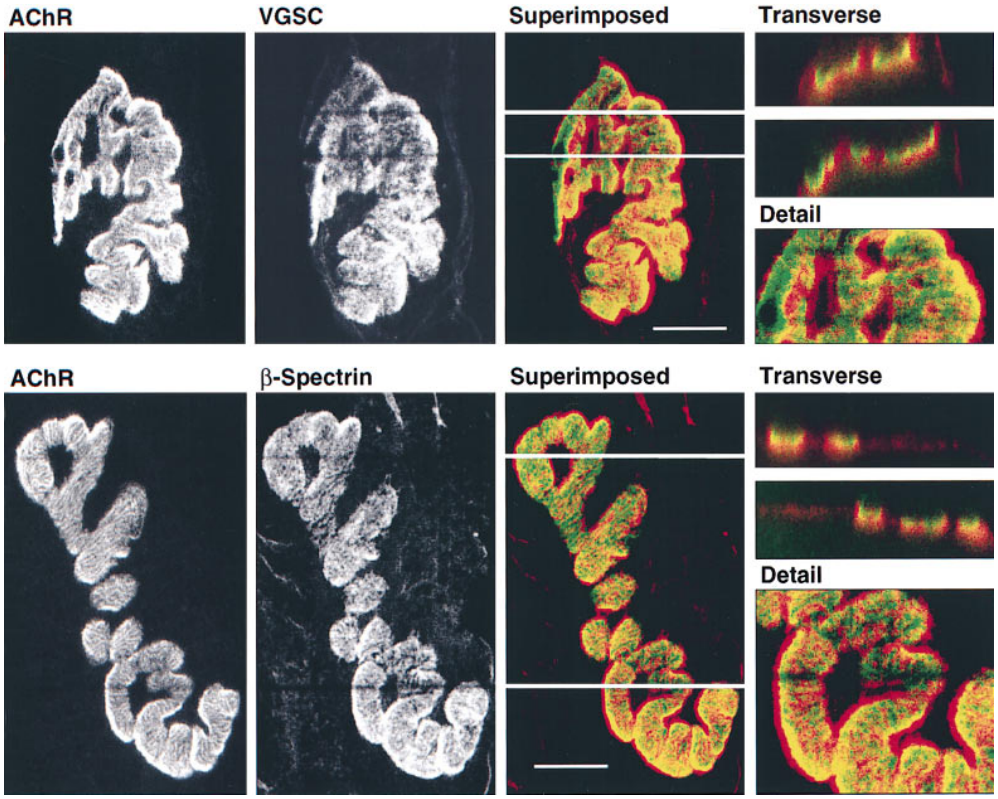

Figure 4. Pseudo-colored confocal micrographs of rat soleus NMJs. Teased fiber preparations were dual labeled with FITC α-BgTx (*green*) to identify AChRs and antibodies to VGSCs (AP 1380) or β-spectrin (RBC2/5C4) visualized with TRITC secondary antibodies (*red*). Both en face and reconstructed transverse views are shown. The superimposed en face images reveal a fringe of VGSC or β-spectrin labeling that extends laterally beyond the AChR labeling (*Superimposed* and *Detail*). Transverse views (at the position of the *white lines*) show that this fringe is also present on the cytoplasmic surface of the AChR domain. This pattern of labeling is consistent with the localization of AChRs at the tops of the postsynaptic folds and of VGSC and β-spectrin in the depths of the folds. Bar, 10 μm.

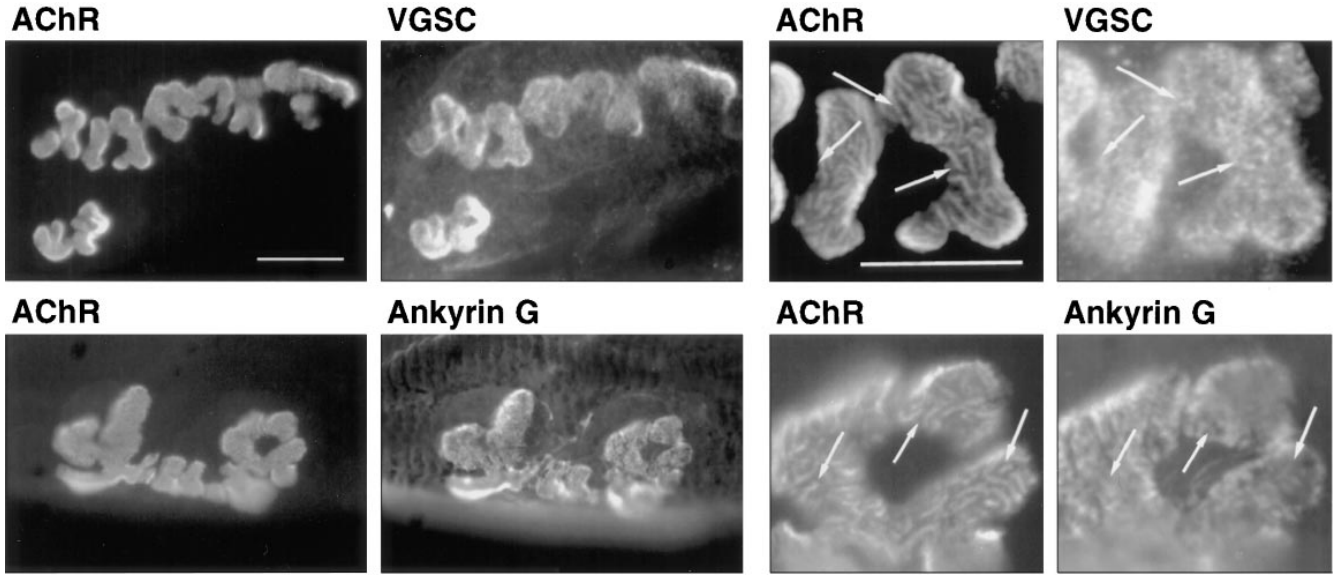

Figure 5. Comparison of the distribution of VGSCs and ankyrin$_G$ with that of AChRs in en face views of the NMJ. Digitized images are shown of teased fiber preparations from rat soleus muscles dual labeled with an antibody to either VGSCs (AP1380) or ankyrin$_G$ (Ank$_G$@SpBd) and FITC α-BgTx to identify AChRs. Low magnification images (×50 objective; Bar, 20 μm) show the overall distribution of immunolabeling at the NMJ. At higher magnification (×100 objective; Bar, 10 μm), arrows highlight areas where AChRs are organized in a linear fashion, whereas VGSCs and ankyrin$_G$ have a more spotty distribution that clearly extends beyond the AChR region.

VGSC immunolabeling having distinctly different spatial distributions. These observations are consistent with a previous study (Flucher and Daniels, 1989) that showed, using EM immunogold labeling, that VGSCs are concentrated in the depths of the postsynaptic folds and largely excluded from the AChR-rich domain at the tops of the folds. Moreover, the pattern of β-spectrin immunolabeling is similar to that of VGSC labeling in both en face views and in reconstructed transverse sections (Fig. 4). This indicates that β-spectrin, like VGSCs, is present in the depths of the postsynaptic folds. An isoform of β-spectrin has previously been reported to be associated with AChRs in myotube cultures and at adult rat NMJs (Bloch and Morrow, 1989). Our results show that an isoform of β-spectrin is present at NMJs, which is clearly associated with VGSC-rich domains and not with AChRs, indicating that there may be multiple β-spectrin isoforms in skeletal muscle.

If ankyrin$_G$ is an intermediary in the binding of VGSCs and β-spectrin at the NMJ then its distribution would be expected to be similar to that of VGSCs. In low magnification en face views of NMJs, immunolabeling for both VGSCs and ankyrin$_G$ is concentrated at the adult NMJ and is approximately codistributed with the AChRs (Fig. 5). On closer examination however, it can be seen that labeling for ankyrin$_G$ extends laterally beyond that for AChRs, as does immunolabeling for VGSCs and β-spectrin (Fig. 4). At higher magnification, differences in the detail of the labeling patterns can be seen (Fig. 5, *arrows*). Whereas AChRs seem to be organized in a characteristic linear pattern corresponding to the crests of the postsynaptic folds, VGSCs and ankyrin$_G$ have a more punctate distribution with some features of the labeling pattern being quite different from that of the AChR labeling. Fig. 5 thus confirms and extends the observations of Flucher and Daniels (1989), which found that VGSCs and ankyrin are localized in the depths of the postsynaptic folds. However, we have used different antibodies, in particular the antibody used here to demonstrate ankyrin labeling is specific for the isoform of ankyrin found at the nodes of Ranvier—ankyrin$_G$ (Kordeli et al., 1995).

To test directly the hypothesis that β-spectrin is colocalized with VGSCs, teased fibers were double labeled with antibodies to VGSCs and with antibodies to the structurally related cytoskeletal proteins β-spectrin, dystrophin, and utrophin (Fig. 6). The distribution of immunolabeling of both β-spectrin and dystrophin was found to be strikingly similar to that of VGSCs (Fig 6, *arrows*). However, occasionally, very slight differences in the fine pattern of dystrophin and VGSC labeling could be detected. In contrast, utrophin immunolabeling was quite different to that of VGSCs, often resembling a more linear pattern similar to that associated with AChR labeling (Fig. 5). These observations suggest that the two distinct ion channel domains occupied by VGSCs and AChRs at the NMJ are matched by distinct cytoskeletal protein domains, with β-spectrin and dystrophin (but not utrophin) being colocalized with VGSCs.

Distribution of VGSCs and Cytoskeletal Proteins in the PJ Region

Electrophysiological and EM labeling studies have suggested that the local high density of VGSCs is not confined to the NMJ but extends into the perijunctional region (Caldwell et al., 1986; Flucher and Daniels, 1989; Le Treut et al., 1990). Therefore, the distribution of VGSCs and cytoskeletal proteins was examined in transverse sections of muscle that allow the entire circumference of the muscle fiber membrane to be examined. Dual labeling confirms that VGSC immunolabeling is concentrated at the NMJ

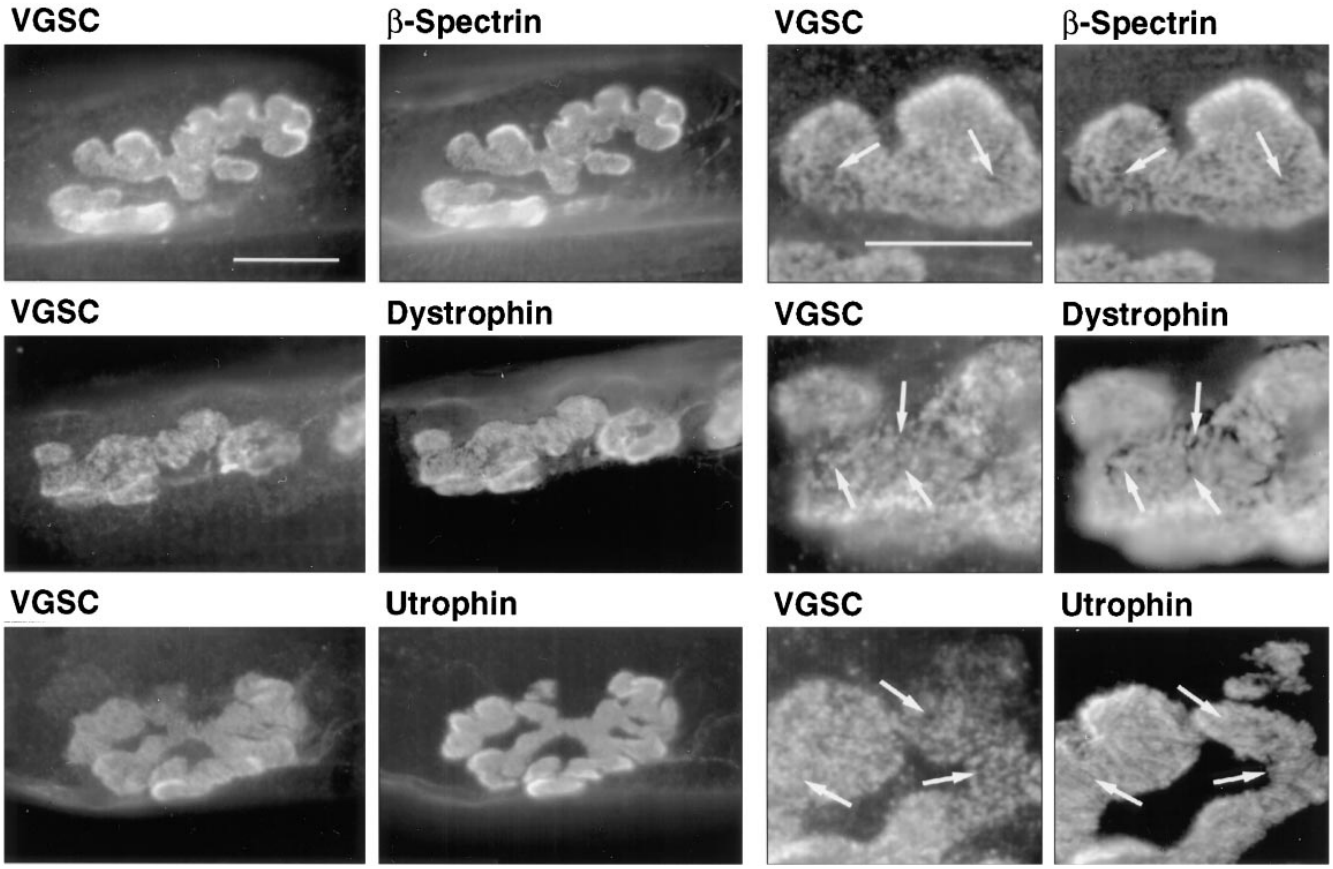

Figure 6. The distribution of VGSCs and the cytoskeletal proteins β-spectrin, dystrophin, and utrophin in en face views of the NMJ. Teased fiber preparations of rat soleus muscles were double labeled with a polyclonal antibody to VGSCs (AP1380; visualized with TRITC secondary antibody), and monoclonal antibodies for β-spectrin (RBC2/5C4), dystrophin (DY8/6C5), and utrophin (DRP3/20C5) all visualized with FITC secondary antibody. Low magnification images (×50 objective; Bar, 20 μm) show the overall distribution of immunolabeling at the NMJ. At higher magnification (×100 objective; Bar, 10 μm), arrows highlight distinctive features of the immunolabeling patterns. Labeling of both β-spectrin and dystrophin resembles the punctate distribution of VGSC immunolabeling at the NMJ. β-Spectrin appears to be precisely colocalized with VGSCs, there are subtle differences in the VGSC and dystrophin distributions whereas VGSCs and utrophin have distinctly different labeling patterns.

(Fig. 7). As expected, VGSC immunolabeling was not uniformly distributed in the rest of the muscle fiber but appeared to be concentrated in regions close to the NMJ. Interestingly, subsequent serial sections through the same NMJ shows that this perijunctional increase in VGSC labeling is matched by increased immunolabeling for β-spectrin but not for dystrophin (Fig. 7, *arrows*). Utrophin immunolabeling acts as a control for the double antibody–labeling technique. Since immunolabeling for utrophin is restricted to the NMJ and to intramuscular blood vessels it can clearly be seen that there is no inappropriate cross-reaction between the antibodies used in this procedure (Fig. 7). These observations suggest that in the perijunctional region, as at the NMJ, the concentration of β-spectrin closely parallels that of VGSCs but the concentration of dystrophin does not.

If VGSC clustering is mediated via an interaction between ankyrin$_G$ and β-spectrin, then ankyrin$_G$ would also be expected to be concentrated at the NMJ and in the perijunctional region. The distribution of ankyrin$_G$ immunolabeling in the muscle fiber membrane was therefore examined and compared with that of the cytoskeletal proteins β-spectrin, utrophin, and dystrophin. Transverse sections were dual labeled with ankyrin$_G$ antibody and BgTx to allow the NMJ to be identified (Fig. 8). Ankyrin$_G$ appeared concentrated at the NMJ and in adjacent regions, compared with extrajunctional regions. Subsequent serial sections were double antibody labeled and revealed that like VGSCs, the perijunctional concentration of ankyrin$_G$ immunolabeling is mirrored by β-spectrin (Fig. 8), but not by dystrophin or utrophin (data not shown). Thus ankyrin$_G$ and β-spectrin are colocalized at the NMJ and in the perijunctional region where the concentration of ankyrin$_G$ appears to parallel that of β-spectrin.

In addition to sarcolemmal immunolabeling, Fig. 8 also reveals the presence of myoplasmic labeling by the ankyrin$_G$ antibody. The specificity of this myoplasmic labeling is confirmed by comparing Figs. 7 and 8, in which double primary antibody labeling is illustrated. In both figures the secondary antibodies used are the same. However, additional labeling of blood vessels is specific to the utrophin antibody (Fig. 7), and myoplasmic labeling is specific to the ankyrin$_G$ antibody (Fig. 8). Devarajan et al. (1996) identified a truncated isoform of ankyrin$_G$, ank$_{G119}$, in kidney

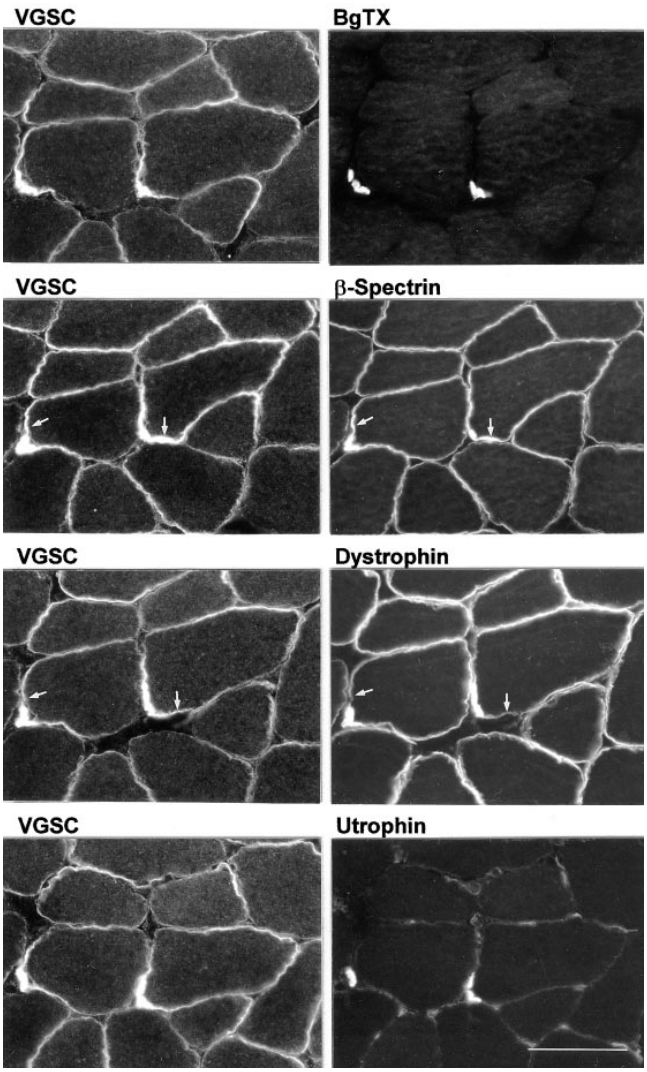

Figure 7. The distribution of VGSCs and the cytoskeletal proteins β-spectrin, dystrophin, and utrophin in rat soleus muscle fibers. Transverse serial sections through the same NMJs were double labeled with a polyclonal antibody to VGSCs (AP1380; visualized with TRITC secondary antibody) and FITC α-BgTx to identify the NMJ, and monoclonal antibodies to β-spectrin (NCLSPEC2), dystrophin (DY8/6C5), and utrophin (DRP3/20C5) visualized with FITC secondary antibody. Immunolabeling for both β-spectrin and dystrophin is codistributed with that for VGSCs in the muscle fiber. In the perijunctional region the concentration of VGSCs parallels that of β-spectrin but not of dystrophin (*arrows*). Utrophin immunolabeling is intense at NMJs (fainter in blood vessels) and serves as a control for the specificity of the secondary antibodies in this double antibody labeling procedure. Bar, 50 μm.

cells that binds spectrin but does not associate with the plasma membrane. Northern blot analysis of the mRNA for this truncated ankyrin$_G$ isoform indicated that this isoform was also present in skeletal muscle (Devarajan et al., 1996). The immunolabeling seen in this study could correspond to this truncated ankyrin$_G$ isoform.

Quantification

To assess the intensity of immunolabeling for VGSCs, ankyrin$_G$, β-spectrin, and dystrophin regions of J, PJ, and XJ labeling were identified in transverse muscle sections (as in Fig. 2). The mean fluorescence labeling intensity per μm^2 in each region was measured and normalized to that in the XJ region (Fig. 9). All the proteins studied are clearly concentrated at the NMJ. The cytoskeletal proteins ankyrin$_G$, β-spectrin, and dystrophin are all increased three- to fourfold, whereas VGSCs are increased sixfold (Fig. 9). The increase in the cytoskeletal proteins is approximately in line with the increase in membrane at the NMJ as a result of postsynaptic folding (Wood and Slater, 1997). The greater increase in VGSCs suggests that there may actually be a higher density of channels per unit area of membrane within the folds at the NMJ than in XJ regions, as suggested previously (Caldwell et al., 1986; Flucher and Daniels, 1989). A highly significant ($P < 0.001$; *t* test) perijunctional increase of 1.5–2-fold was seen for VGSCs, ankyrin$_G$, and β-spectrin, but not for dystrophin (Fig. 9). This analysis indicates that the concentration of β-spectrin closely parallels that of VGSCs and ankyrin$_G$ in the PJ region, but that the concentration of dystrophin does not.

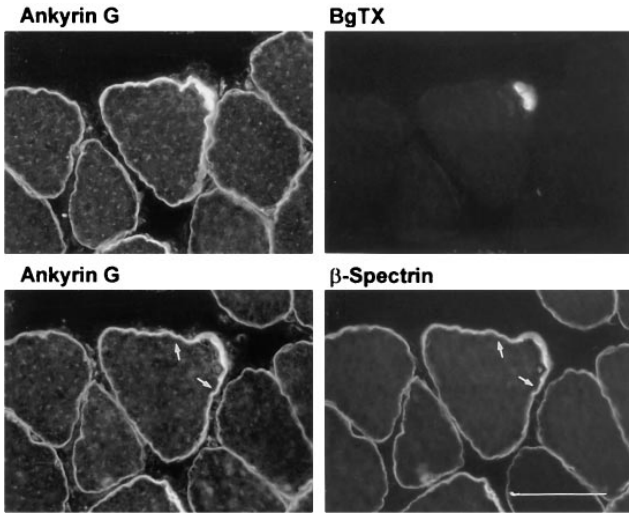

Figure 8. The distribution of ankyrin$_G$ and β-spectrin in rat soleus muscle fibers. Transverse serial sections through the same NMJ were double labeled with a polyclonal antibody to ankyrin$_G$ (Ank$_G$@SpBd; visualized with TRITC-secondary antibody), and FITC α-BgTx to identify the NMJ, and monoclonal antibody for β-spectrin (NCLSPEC2) visualized with FITC secondary antibody. β-Spectrin and ankyrin$_G$ are concentrated at the NMJ and in perijunctional regions (*arrows*). Immunolabeling for ankyrin$_G$ is also seen in the myoplasm. Bar, 50 μm.

Distribution of VGSC in the Absence of Dystrophin

Dystrophin and VGSCs are colocalized at the NMJ and throughout the muscle fiber membrane. Although there is no increase in dystrophin immunolabeling in the PJ region, it is still present there. To test for a possible influence of dystrophin in maintaining the high concentration of VGSCs at the NMJ, the distribution of VGSCs was examined in muscles from the *mdx* mouse, in which a point mutation on the X chromosome results in a profound deficiency of dystrophin (Sicinski et al., 1989). Transverse sections of ETA muscles from control and *mdx* mice were

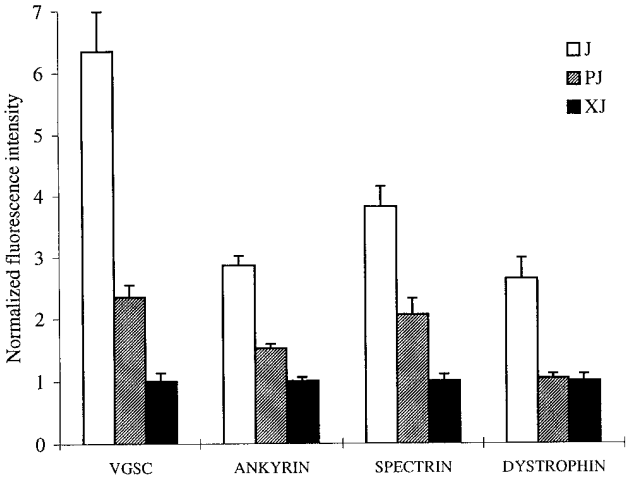

Figure 9. Comparison of intensity of immunofluorescent labeling for VGSCs, ankyrin$_G$, β-spectrin, and dystrophin in junctional (*J*), perijunctional (*PJ*), and extrajunctional (*XJ*) regions of rat soleus muscle fiber membrane. The mean fluorescence intensity of immunolabeling, normalized to XJ, is shown for each protein/antibody. J labeling for VGSCs (AP1380) is increased sixfold whereas labeling for ankyrin$_G$ (Ank$_G$@SpBd), β-spectrin (NCLSPEC2), and dystrophin (DY8/6C5) is increased two- to threefold. PJ labeling is increased 1.5–2-fold for all proteins except dystrophin. Each point is the mean ± SEM of observations in 20 muscle fibers from two soleus muscles.

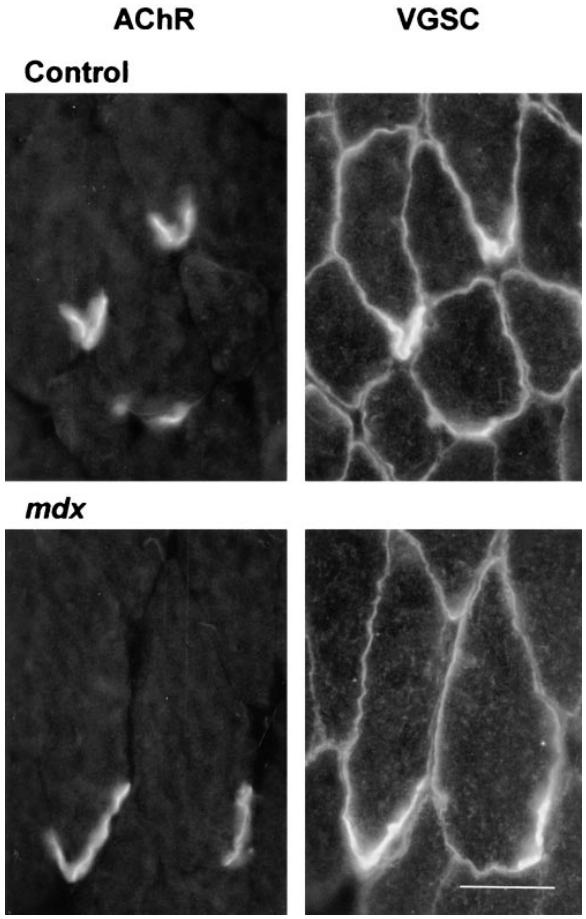

Figure 10. Clustering of VGSCs at the NMJ of dystrophin deficient *mdx* mouse ETA muscle. Transverse sections of control and *mdx* ETA muscle were dual labeled with VGSC antibody (AP-1380) visualized with TRITC secondary antibody and FITC α-BgTx, which allows NMJs to be identified. VGSCs are obviously clustered at the NMJ and in perijunctional regions in the absence of dystrophin. Bar, 20 μm.

dual labeled with BgTx, to identify the NMJs and the VGSC antibody. Both in the presence and absence of dystrophin, VGSC immunolabeling was clearly concentrated at the NMJ and in PJ regions of mouse muscle (Fig. 10). This observation indicates that dystrophin does not play an essential role in clustering VGSCs at the NMJ in adult muscle.

Discussion

The main finding of this study is that at adult rat NMJs, β-spectrin is colocalized with both VGSCs and ankyrin$_G$. Flucher and Daniels (1989) used EM immunogold labeling to show that VGSCs are concentrated in the depths of the postsynaptic folds, whereas AChRs are restricted to the tops of the folds. We have demonstrated that these two ion channel domains can be distinguished in en face views of labeled NMJs. Confocal microscopy of immunolabeled teased fibers has shown that β-spectrin is clearly associated with VGSC-rich domains in the depths of the postsynaptic folds and not colocalized with AChRs. Furthermore, within the NMJ, the punctate pattern of labeling for VGSCs is mirrored by β-spectrin and by ankyrin$_G$. This contrasts to the linear arrays of labeling for AChRs and utrophin, which are thought to correspond to the tops of the postsynaptic folds. The punctate labeling pattern may arise from the branching of the folds and their poor alignment with the fold openings or from the presence of VGSC microclusters within the fold membrane. In addition, we have shown that the concentration of VGSCs in perijunctional regions is paralleled by increases in the concentration of both β-spectrin and ankyrin$_G$. The precise colocalization of β-spectrin and ankyrin$_G$ with VGSCs at the NMJ and in perijunctional regions suggests that these three proteins may interact with one another to provide a means of maintaining a high density of VGSCs at the NMJ.

The muscle cytoskeletal protein dystrophin, a member of the spectrin family, has previously been shown to have a similar distribution to that of β-spectrin at the NMJ (Bewick et al., 1992). Likewise, in this study dystrophin has a somewhat punctate distribution at the NMJ that extends beyond the AChR-labeled regions, suggestive of a localization in the depths of the postsynaptic folds. However, examination of the labeling pattern of VGSCs and dystrophin in greater detail revealed subtle differences. Furthermore, although dystrophin is concentrated at the NMJ, it is not increased in the perijunctional region. Finally, in muscles of the *mdx* mouse (which lacks dystrophin), VGSCs are normally distributed and concentrated at the NMJ. Together, these observations suggest that dystrophin does not play a significant role in clustering VGSCs at the NMJ.

Syntrophin, a protein closely associated with dystrophin and utrophin, contains PSD-95, DIgA, ZO-1–like (PDZ) domains that in other situations have been implicated in

clustering of ion channels (Kim et al., 1995). Recently it has been reported that VGSCs copurify with syntrophin and dystrophin in skeletal and cardiac muscle (Gee et al., 1998). In the *mdx* mouse, which lacks dystrophin, syntrophin and other dystrophin-associated proteins are greatly reduced in abundance in the XJ region of the muscle fiber but they persist at the NMJ, presumably in association with utrophin (Matsumura et al., 1992). Although we have shown that the distribution of VGSCs in *mdx* mouse muscle is essentially normal, it remains possible that interactions with syntrophin represent an additional means of localizing VGSCs at the NMJ.

VGSC Concentration at the NMJ

The concentration of VGSCs in J and PJ regions is likely to be functionally important. The action potential threshold at the NMJ is lower than in extrajunctional regions (Wood and Slater, 1995) and the high safety factor for neuromuscular transmission may be attributed in part to the postsynaptic folds and the VGSCs concentrated within them (Wood and Slater, 1997). Various approaches have been used to estimate the number of VGSCs at the NMJ. Electrophysiological analyses using loose-patch voltage-clamp recording to measure sodium current density have suggested that the density of VGSCs at the NMJ was 8,000/μm^2 in rat muscle (Caldwell et al., 1986), representing a 20-fold increase over XJ sodium current densities. This estimate of channel number was based on values of sodium current density and related to VGSC-specific toxin binding studies of the nodes of Ranvier. It was complicated by huge variations in sodium current density within the NMJ and by uncertainties concerning the amount of folded membrane in the patch examined. An alternative approach of EM autoradiography, using radiolabeled scorpion toxins, has subsequently suggested that there is a sevenfold increase in VGSC concentration at the NMJ compared with XJ regions (Le Treut et al., 1990), and that this may correspond to as many as 5,000 channels per μm^2 in the fold membrane (Boudier et al., 1992).

In this study, we have used the intensity of fluorescent labeling as a measure of VGSC density. Whereas this approach does not lead to a measure of the absolute number of VGSCs per unit area, it is useful in providing an indication of the density of VGSC labeling within the NMJ relative to that in other parts of the same muscle fiber. Using this approach, we have found that the intensity of VGSC labeling is sixfold greater at the NMJ than in XJ regions. Since VGSCs are localized in the postsynaptic folds, the folding itself is likely to account for much of this increase. Folding results in a fivefold increase in the postsynaptic membrane area at the rat soleus NMJ (Wood and Slater, 1997). However, not all of that folded membrane is occupied by VGSCs. The boundary between the regions of high AChR and VGSC density occurs about one-third of the way into the folds (Flucher and Daniels, 1989). This suggests that the actual increase in the amount of membrane that accommodates VGSCs is about threefold, consistent with the degree of increased labeling of β-spectrin, ankyrin$_G$, and dystrophin, which all appear to occupy the same region of the folds as VGSCs. Thus the sixfold junctional increase in VGSC labeling indicates that the junctional VGSC density per unit area is at least twice that in extrajunctional membrane and that the increase in VGSCs is clearly more than that for cytoskeletal proteins. Whereas our value for the increase in local VGSC density is lower than previous estimates, there are substantial uncertainties associated with all the methods used.

In the perijunctional region there are no folds, yet several studies have suggested that VGSCs are also concentrated in the perisynaptic region. Electrophysiological studies suggest that the perijunctional density is 5–10-fold greater than that in the extrajunctional region (Beam et al., 1985; Caldwell et al., 1986), whereas EM studies suggest that the junctional increase in VGSCs extends into the perijunctional region (Le Treut et al., 1990; Boudier et al., 1992). The observations reported here suggest that the density of VGSCs in the perijunctional region is 2.5-fold greater than in the extrajunctional region, and is thus similar to that within the postsynaptic folds at the NMJ. This increased VGSC density in the perisynaptic region may function to ensure the initial spread of depolarization away from the endplate.

VGSC Clustering and Cytoskeletal Proteins

The factors leading to the increased density of VGSCs at the NMJ are poorly understood. One possibility is that VGSCs are preferentially synthesized and inserted into the membrane in the junctional region. It is well known that the genes for AChRs and AChE are preferentially synthesized by postsynaptic myonuclei (Brenner et al., 1990; Jasmin et al., 1993; Duclert and Changeux, 1995), and recent reports indicate that this is also true for a number of other postsynaptic molecules including neural cell adhesion molecule, rapsyn, s-laminin (Moscoso et al., 1995), and utrophin (Gramolini et al., 1997; Vater et al., 1988). If there is preferential expression of VGSC genes at the NMJ, then the high concentration of VGSCs at the NMJ and in perijunctional regions might well result from a gradient of mRNA concentration with its peak at the NMJ. However, NMJ-specific gene expression is unlikely to be the entire explanation for the observations reported. It seems probable that local mechanisms must also exist to regulate the placement of ion channels at the NMJ since AChRs, which exhibit synapse-specific gene expression, are not found in perijunctional regions.

One influence on VGSC distribution and concentration at the NMJ is likely to be interaction with the underlying cytoskeleton. Here we have shown very close spatial associations between VGSCs and both β-spectrin and ankyrin$_G$. Studies in nerve cells (Srinivasan et al., 1988; Kordeli et al., 1990; Joe and Angelides, 1992; Kaplan et al., 1997) have led to the idea that ankyrin$_G$ links VGSCs to the underlying spectrin-based cytoskeleton and that this helps to maintain the high local density of ion channels. Whereas such a general model seems plausible for the NMJ, many of the details remain uncertain. For example, the observations of this study suggest that the local density of VGSCs is increased more within the folds than that of β-spectrin and ankyrin$_G$. Any interpretation of this depends on knowledge of the likely stoichiometric relationships between these three proteins. At present it is not clear that every VGSC must bind to one ankyrin$_G$ molecule or that one

ankyrin$_G$ would have to bind to one β-spectrin molecule for VGSCs to become localized to the membrane. Since ankyrin is known to be capable of binding more than one ion channel at a time (Michaely and Bennett, 1995), it is possible that individual ankyrin$_G$ molecules would bind multiple VGSCs. Furthermore, it is not clear what fraction of β-spectrin molecules have ankyrin$_G$ bound to them or that this is the same in J, PJ, or XJ regions of the muscle fiber surface. Thus, although the observations of this study show highly suggestive parallels in the density of VGSCs, ankyrin$_G$, and β-spectrin, the full significance of these remains uncertain.

The precise colocalization of β-spectrin with both VGSCs and ankyrin$_G$ at the NMJ suggests that interactions between these proteins play a role in the localization of VGSCs in muscle. Such a model has been proposed to account for the local high density of VGSCs at axon hillocks and initial segments, and at the nodes of Ranvier (Waxman and Ritchie, 1985; Wollner and Catterall, 1986; Srinivasan et al., 1988; Kordeli et al., 1990; Dugandzija-Novakovic et al., 1995; Kaplan et al., 1997). Our findings in skeletal muscle suggest that VGSC–ankyrin$_G$–β-spectrin interactions may be common to all excitable cells where VGSCs are found at high density.

We are grateful to Drs. R. Levinson, S. Lambert, and L. Anderson for generous gifts of antibodies. We thank C. Young for her assistance with producing the figures and T. Booth for his assistance with confocal microscopy.

This project was supported by grants from the Muscular Dystrophy Group of Great Britain and the Myasthenia Gravis Association.

Received for publication 10 June 1997 and in revised form 5 December 1997.

References

Angelides, K.J. 1986. Fluorescently labeled Na^+ channels are localized and immobilized to synapses of innervated muscle fibers. *Nature.* 321:63–66.

Angelides, K.J., L.W. Elmer, D. Loftus, and E. Elson. 1988. Distribution and lateral mobility of voltage-dependent sodium channels in neurons. *J. Cell Biol.* 106:1911–1925.

Apel, E.D., and J.P. Merlie. 1995. Assembly of the postsynaptic apparatus. *Curr. Opin. Neurobiol.* 5:62–67.

Beam, K.G., J.H. Caldwell, and D.T. Campbell. 1985. Na channels in skeletal muscle concentrated near the neuromuscular junction. *Nature.* 313:588–590.

Bennett, V. 1990. Spectrin-based membrane skeleton: a multipotential adaptor between plasma membrane and cytoplasm. *Physiol. Rev.* 70:1029–1065.

Bennett, V., and D.M. Gilligan. 1993. The spectrin-based membrane cytoskeleton and micron-scale organization of the plasma membrane. *Annu. Rev. Cell Biol.* 9:27–66.

Betz, W.J., J.H. Caldwell, and S.C. Kinnamon. 1984. Increased sodium conductance in the synaptic region of rat skeletal muscle fibres. *J. Physiol. (Lond.).* 352:189–202.

Bewick, G.S., L.V.B. Nicholson, C. Young, E. O'Donnell, and C.R. Slater. 1992. Different distributions of dystrophin and related proteins at nerve-muscle junctions. *Neuroreport.* 3:857–860.

Bewick, G.S., L.V.B. Nicholson, C. Young, and C.R. Slater. 1993. Relationship of a dystrophin-associated glycoprotein to junctional acetylcholine receptor clusters in rat skeletal muscle. *Neuromuscul. Disord.* 3:503–506.

Bloch, R.J., and J.S. Morrow. 1989. An unusual β-spectrin associated with clustered acetylcholine receptors. *J. Cell Biol.* 108:481–493.

Boudier, J.L., T. Le Treut, and E. Jover. 1992. Autoradiographic localization of voltage-dependent sodium channels on the mouse neuromuscular junction using ^{125}I-α scorpion toxin. II. Sodium channel distribution on postsynaptic membranes. *J. Neurosci.* 12:454–466.

Brenner, H.R., V. Witzemann, and B. Sakmann. 1990. Imprinting of acetylcholine receptor messenger RNA accumulation in mammalian neuromuscular synapses. *Nature.* 344:544–547.

Caldwell, J.H., D.T. Campbell, and K.G. Beam. 1986. Na channel distribution in vertebrate skeletal muscle. *J. Gen. Physiol.* 87:907–932.

Devarajan, P., P.R. Stabah, A.S. Mann, T. Ardito, M. Kashgarian, and J.S. Morrow. 1996. Identification of a small cytoplasmic ankyrin (Ank$_{G119}$) in the kidney and muscle that binds βIΣ* spectrin and associates with the Golgi apparatus. *J. Cell Biol.* 133:819–830.

Duclert, A., and J.P. Changeux. 1995. Acetylcholine receptor gene expression at the developing neuromuscular junction. *Physiol. Rev.* 75:339–368.

Dugandzija-Novakovic, S., A.G. Koszowski, S.R. Levinson, and P. Shrager. 1995. Clustering of Na^+ channels and node of Ranvier formation in remyelinating axons. *J. Neurosci.* 15:492–503.

Flucher, B.E., and M.P. Daniels. 1989. Distribution of Na^+ channels and ankyrin in neuromuscular junctions is complementary to that of acetylcholine receptors and the 43 kd protein. *Neuron.* 3:163–175.

Gee, S.H., R. Madhaven, S.R. Levinson, J.H. Caldwell, R. Sealock, and S.C. Froehner. 1998. Interaction of muscle and brain sodium channels with multiple members of the syntrophin family of dystrophin-associated proteins. *J. Neurosci.* 18:128–137.

Gramolini, A.O., C.L. Dennis, J.M. Tinsley, G.S. Robertson, J. Cartaud, K.E. Davies, and B.J. Jasmin. 1997. Local transcriptional control of utrophin expression at the neuromuscular synapse. *J. Biol. Chem.* 272:8117–8120.

Haimovich, B., D.L. Schotland, W.E. Fieles, and R.L. Barchi. 1987. Localization of sodium channel subtypes in adult rat skeletal muscle using channel-specific monoclonal antibodies. *J. Neurosci.* 7:2957–2966.

Jasmin, B.J., R.K. Lee, and R.L. Rotundo. 1993. Compartmentalization of acetylcholinesterase mRNA and enzyme at the vertebrate neuromuscular junction. *Neuron.* 11:467–477.

Joe, E., and K. Angelides. 1992. Clustering of voltage-dependent sodium channels on axons depends on Schwann cell contact. *Nature.* 356:333–335.

Kaplan, M.R., A. Meyer-Franke, S. Lambert, V. Bennett, I.D. Duncan, S.R. Levinson, and B.A. Barres. 1997. Induction of sodium channel clustering by oligodendrocytes. *Nature.* 386:724–728.

Kim, E., M. Niethammer, A. Rothschild, Y.N. Jan, and M. Sheng. 1995. Clustering of Shaker-type K^+ channels by interaction with a family of membrane-associated guanylate kinases. *Nature.* 378:85–88.

Kordeli, E., and V. Bennett. 1991. Distinct ankyrin isoforms at neuron cell bodies and nodes of Ranvier resolved using erythrocyte ankyrin-deficient mice. *J. Cell Biol.* 114:1243–1259.

Kordeli, E., J. Davis, B. Trapp, and V. Bennett. 1990. An isoform of ankyrin is localized at nodes of Ranvier in myelinated axons of central and peripheral nerves. *J. Cell Biol.* 110:1341–1352.

Kordeli, E., S. Lambert, and V. Bennett. 1995. AnkyrinG. A new ankyrin gene with neural-specific isoforms localized at the axonal initial segment and node of Ranvier. *J. Biol. Chem.* 270:2352–2359.

Lambert, S., and V. Bennett. 1993. From anaemia to cerebellar dysfunction. A review of the ankyrin gene family. *Eur. J. Biochem.* 211:1–6.

Le Treut, T., J.L. Boudier, E. Jover, and P. Cau. 1990. Localization of voltage-sensitive sodium channels on the extrasynaptic membrane surface of mouse skeletal muscle by autoradiography of scorpion toxin binding sites. *J. Neurocytol.* 19:408–420.

Matsumura, K., J.M. Ervasti, K. Ohlendieck, S.D. Kahl, and K.P. Campbell. 1992. Association of dystrophin-related protein with dystrophin-associated proteins in *mdx* mouse muscle. *Nature.* 360:588–591.

Michaely, P., and V. Bennett. 1995. The ANK repeats of erythrocyte ankyrin form two distinct but cooperative binding sites for the erythrocyte anion exchanger. *J. Biol. Chem.* 270:22050–22057.

Moscoso, L.M., J.P. Merlie, and J.R. Sanes. 1995. N-CAM, 43K-rapsyn, and S-laminin mRNAs are concentrated at synaptic sites in muscle fibers. *Mol. Cell. Neurosci.* 6:80–89.

Ohlendiek, K., J.M. Ervasti, K. Matsumura, S.D. Kahl, C.J. Leveille, and K.P. Campbell. 1991. Dystrophin-related protein is localized to neuromuscular junctions of adult skeletal muscle. *Neuron.* 7:499–508.

Sealock, R., M.H. Butler, N.R. Kramarcy, K.-X. Gao, A.A. Murnane, K. Douville, and S.C. Froehner. 1991. Localization of dystrophin relative to acetylcholine receptor domains in electric tissue and adult and cultured skeletal muscle. *J. Cell Biol.* 113:1133–1144.

Sicinski, P., Y. Geng, A.S. Ryder-Cook, E. Barnard, M. Darlison, and P. Barnard. 1989. The molecular basis of muscular dystrophy in the mdx mouse is a point mutation. *Science.* 244:1578–1580.

Srinivasan, Y., L. Elmer, J. Davis, V. Bennett, and K. Angelides. 1988. Ankyrin and spectrin associate with voltage-dependent sodium channels in brain. *Nature.* 333:177–180.

Vater, R., C. Young, L.V.B. Anderson, S. Lindsay, D.J. Blake, K.E. Davies, R. Zuellig, and C.R. Slater. 1998. Utrophin mRNA expression in muscle is not restricted to the neuromuscular junction. *Mol. Cell. Neurosci.* In press.

Waxman, S.G., and J.M. Ritchie. 1985. Organization of ion channels in the myelinated nerve fibre. *Science.* 228:1502–1507.

Wollner, D.A., and W.A. Catterall. 1986. Localization of sodium channels in axon hillocks and initial segments of retinal ganglion cells. *Proc. Natl. Acad. Sci. U.S.A.* 83:8424–8428.

Wood, S.J., and C.R. Slater. 1995. Action potential generation in rat slow- and fast-twitch muscles. *J. Physiol. (Lond.).* 486:401–410.

Wood, S.J., and C.R. Slater. 1997. The contribution of postsynaptic folds to the safety factor for neuromuscular transmission in rat fast- and slow-twitch muscles. *J. Physiol. (Lond.).* 500:165–176.

Yeadon, J.E., H. Lin, S.M. Dyer, and S.J. Burden. 1991. Dystrophin is a component of the subsynaptic membrane. *J. Cell Biol.* 115:1069–1076.